Implementation of non-standard tests at powered roof support testing stands in KOMAG

IOP Conf. Series: Earth and Environmental Science **261** (2019) 012028 doi:10.1088/1755-1315/261/1/012028

Implementation of non-standard tests at powered roof support testing stands in KOMAG

W Madejczyk and S Szweda

KOMAG Institute of Mining Technology, 37 Pszczyńska Street, 44-101 Gliwice, Poland

E-mail: sszweda@komag.eu

Abstract: Examples of broadening the scope of application of the unique test stands, originally dedicated to conducting functionality, kinematic and strength tests of powered roof support. Test cycle of bridge bearings load capacity is discussed. The obtained results were used during the certification process of the bearings. The method of testing the strength of welded rails as well as the tests procedure and the results of stiffness tests of the folding metal scaffoldings is given.

1. Introduction

Tests of powered roof support at the KOMAG Laboratory of Tests are conducted in two test stands. At present they are mainly used for tests confirming compliance with the normative requirements by newly designed, modernised or already used powered roof supports which are inspected before being installed at a new longwall face. [1].

Test stand for testing the strength of powered roof support (figure 1), enables loading it in the vertical plane, with an external force of up to 16 MN and a force of up to 4.5 MN in the horizontal plane. The maximum distance of the movable roof of the stand from its floor is 4.8 m. The floor length is 5.1 m and the roof length 7 m.

Test stand for kinematic and functionality tests of the powered roof support (figure 2) can be loaded with a force of up to 10 MN, with a maximum tilting angle of the stand of up to 90°. The maximum distance of the movable roof of the stand from its floor is 4 m. The roof width is 5 m and the length 7.2 m.

The test procedures implemented at these stands are consistent with the PCA [2] accreditation, which defines both the fixed scope and the flexible scope of the tests.

The technical parameters of the test stands, in particular the volume of the generated load acting on the powered roof support and the overall dimensions of the tested object make it relatively easy to adapt these stands to strength tests of other technical devices or to carry out tests of a cognitive nature that go beyond the normative requirements.

Figure 1. Test stand for strength tests of powered roof support [3].

Figure 2. Test stand for kinematic and functionality tests of powered roof support [3].

Examples of implementation of such non-standard tests, significantly extending the testing program carried out at the KOMAG Laboratory of are presented.

2. Testing of bridge bearings

The subject of tests carried out at the test stand for testing strength of powered roof support were the steel spherical bridge bearings of type KPRM [4], multi-directionally sliding, shown schematically in figure 3.

The purpose of bridge bearing tests was to check the conformity of this product with the requirements of the following reference documents:

- PN-EN 1337-7:2003 Structural bearings Part 7: Spherical and cylindrical PTFE bearings [5],
- PN-EN 1337-2:2005 Structural bearings Part 2: Sliding elements [6],
- PN-EN 1337-1:2003 Structural bearings Part 1: General provisions[7],

Test program included the following stages:

- Stage I - checking the load bearing vertical capacity of the bearings;
- Stage II - checking the turning possibility; Etap II – sprawdzenie możliwości obrotu;
- Stage III - determination of the friction coefficient of the sliding element.

Procedure and results of the tests are presented on the example of testing of spherical type steel KPRM bridge bearings, multi-directionally sliding, marked S5.3. Technical parameters of the bearing are summarized in table 1.

2.1. Stage I – testing the bearing load capacity

Checking the surface condition of PTFE (Polytetrafluoroethylene) sheets and bearing sliding surfaces after loading it with vertical force equal to the design load capacity of the serviceability limit states (SLS) was the test objective.

The bearing was placed in a stand on concrete transition plates (7) between the steel pressure plates (2) and (3) (figure 4).

The vertical bearing load determined by the transducers (5) was set by increasing the monotonic pressure in the vertical cylinders of the movable roof of the stand (6) up to the value of 5750 kN, after which the pressure in the roof cylinders was kept constant for about 50 seconds. Then they were gradually reduced until the bearing was completely relieved.

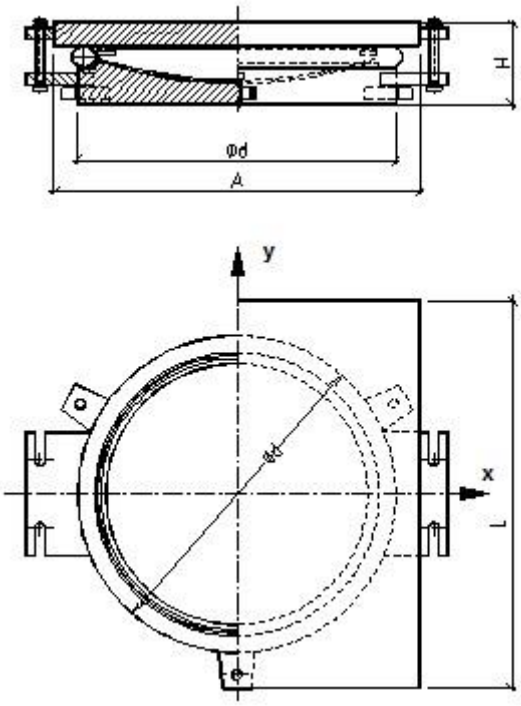

Figure 3. Diagram of tested bridge bearing.

Table 1. Technical parameters of S5.3 bearing

Parameter	Unit	Value
Advance Δ_x (see figure 3)	mm	± 50
Advance Δ_y (see figure 3)	mm	± 25
Angle of rotation	rad	0,02
Design resistance of SLS bearing	kN	5 378
Minimum vertical force at which ULS condition is met	kN	763
Bottom plate diameter, $\varnothing_d$	mm	485
Upper plate width, A	mm	500
Upper plate length, L	mm	$560^{\pm 50}$
Bearing height, H	mm	116
Bearing weight	kg	222

During the test, time curves of bearing load force and ambient temperature (figure 5) were recorded. After testing, the bearing was disassembled and the surface condition of PTFE sheets and sliding surfaces were checked. The view of the PTFE sheets of the lens and the bearing bottom plate after the tests are shown in figure 6 and 7.

In a result of the visual inspection, the surface condition of PTFE sheets and sliding surfaces was found to be correct. Permanent deformation of PTFE sheets also did not occur.

2.2. Stage II – testing the turning possibility

Checking if the metal surface accompanying the PTFE material completely covers the PTFE sheet with the largest turn of the bearing elements against each other and whether the contact between the upper and lower bearing part or any other metal element is met was the test objective.

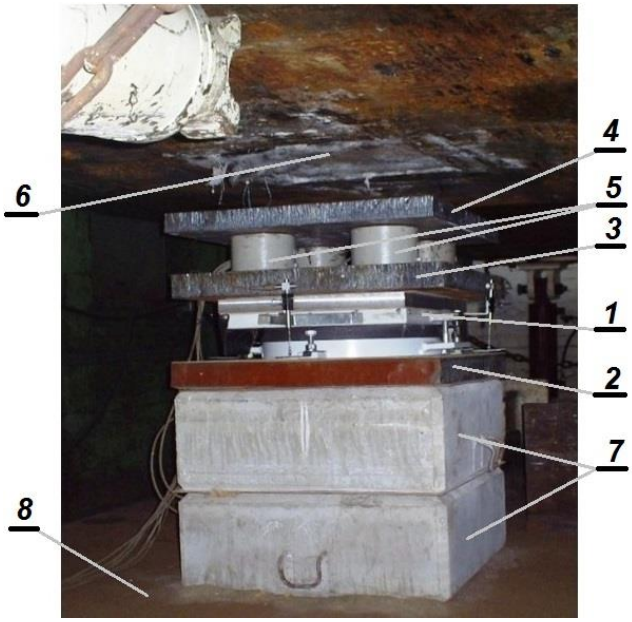

Figure 4. Testing the bridge bearing load capacity – general view of the stand. 1 – tested bearing; 2, 3, 4 – pressure plates; 5 – force transducers; 6 – stand roof; 7 – concrete transition plates, 8 – stand floor.

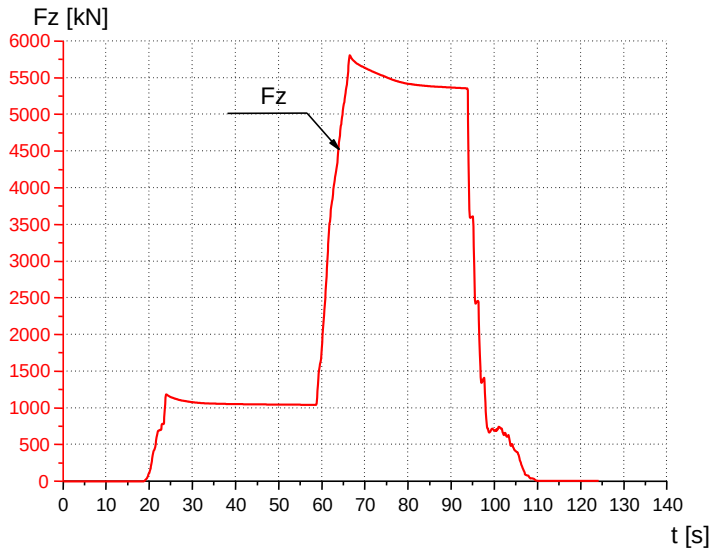

Figure 5. Time curve of force loading the bearing.

The view of bearings arrangement, prepared for testing, is shown in figure 8. Between the two bearings (1), the transitional concrete plates (8) and the steel lever (9) are placed with the upper plates facing each other. The pressure plate (2) rests on the stand floor, while the pressure plate (4), during the test, is loaded with the pressure of the stand roof. Rotation of the bearing components relative to one another, was obtained by pressing on the lever (9) with the force F_5 generated by the cylinder (7) and recorded by the dynamometer (6).

Figure 6. View of the PTFE sheet of lens after bearing capacity test.

Figure 7. View of the PTFE sheet of the bottom plate after bearing capacity test.

The C6 200t HOTTINGER class 0.5 (4 pieces) strain gauge force transducers (5), were set in a square area between the steel plates (3) and (4), above the upper bearing.

Two W20 HOTTINGER class 0.4 (not visible in figure 6) inductive displacement transducers, were placed in the rotation of the bearing at a distance of 400 mm from its vertical axis of symmetry.

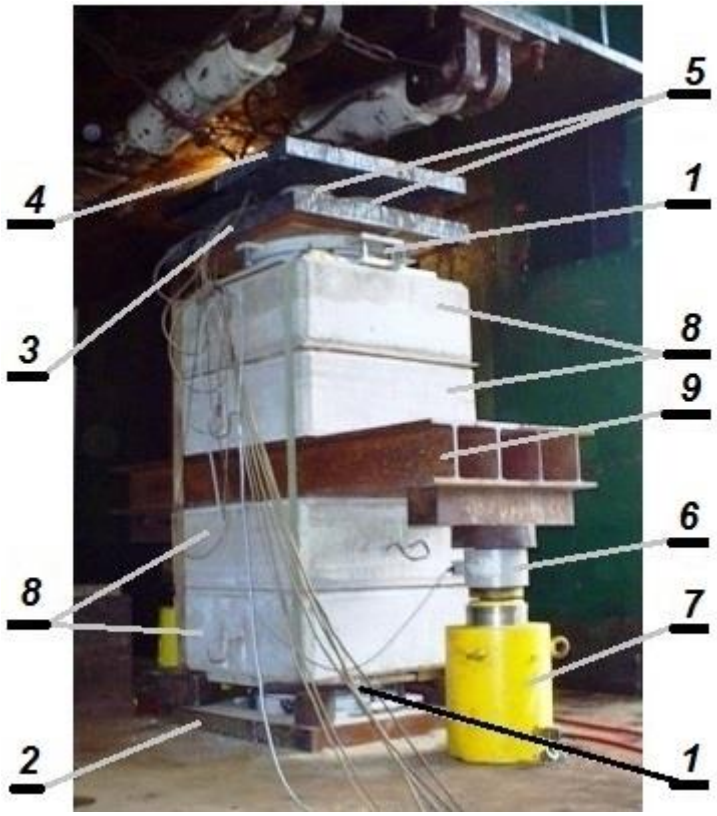

Figure 8. View of the bearing system during the test of rotation and determination of the coefficient of friction on the curved surface. 1 – tested bridge bearing; 2, 3, 4 – pressure plates; 5 – force transducers; 6 – dynamometer; 7 – cylinder; 8 – concrete transition plates.

The vertical load was exerted on the stand roof. Its maximum value reached 4300 kN, which is about 80% of the maximum design load capacity. The maximum rotation angle of the bearing, determined on the basis of displacement transducer readings, was 0.0255 rad, i.e. it was greater than the nominal rotation angle (table 1).

After the test, the bearings were dismantled and examined. As a result of the inspection, it was found that the tested bearing meets the requirements as the metal surface accompanying the PTFE material completely covered the PTFE sheet. There were also no traces of contact between the upper and lower part of the bearing or with any other metal element.

2.3. Stage III – determination of friction coefficient for sliding component of a bearing

2.3.1. Determination of friction coefficient on a curved surface. The test was carried out using the bearing system shown in figure 8. It consisted in measuring the F_5 force generating the bearing (upper) movement at a given vertical load F_z.

Results of the measurements show that the static friction coefficient of a bearing curved components is within the range [0.0293; 0,0522]. Thus, the tested bearing meets the requirements of the standard [6], because the determined friction coefficient has a value of less than 0.06.

2.3.2. Determination of friction coefficient on a flat surface. Two bridge bearings (1) adjacent to each other by upper plates are the test objective. View of arrangement of bearings in the stand is shown in figure 9.

Figure 9. View of arrangement of bearings during determination of friction coefficient on a flat surface 1 – tested bearings; 2, 5 – pressure plates; 3 – transition plate; 4 – transducers; 6 – horizontal cylinder

Bearings, placed between the plates (2), are positioned on a concrete transition plate (3). The vertical bearing load is measured by the transducers (4) placed between the plates (5). The relative displacement of the upper bearing plates (1) is caused by the horizontal force F_6, generated by the cylinder (6).

Time curves: relative displacement l_1, horizontal force F_6 and vertical load bearing F_z are shown in figure 10.

The friction coefficient was determined at different values of normal stress on the upper bearing plates. For example, its value was within the range of [0.0100; 0.0122], at a normal stress of 8.5 MPa.

Carried out measurements, show that the tested bridge bearings meet the requirements of the standard [6] in relation to the friction coefficient on flat surfaces.

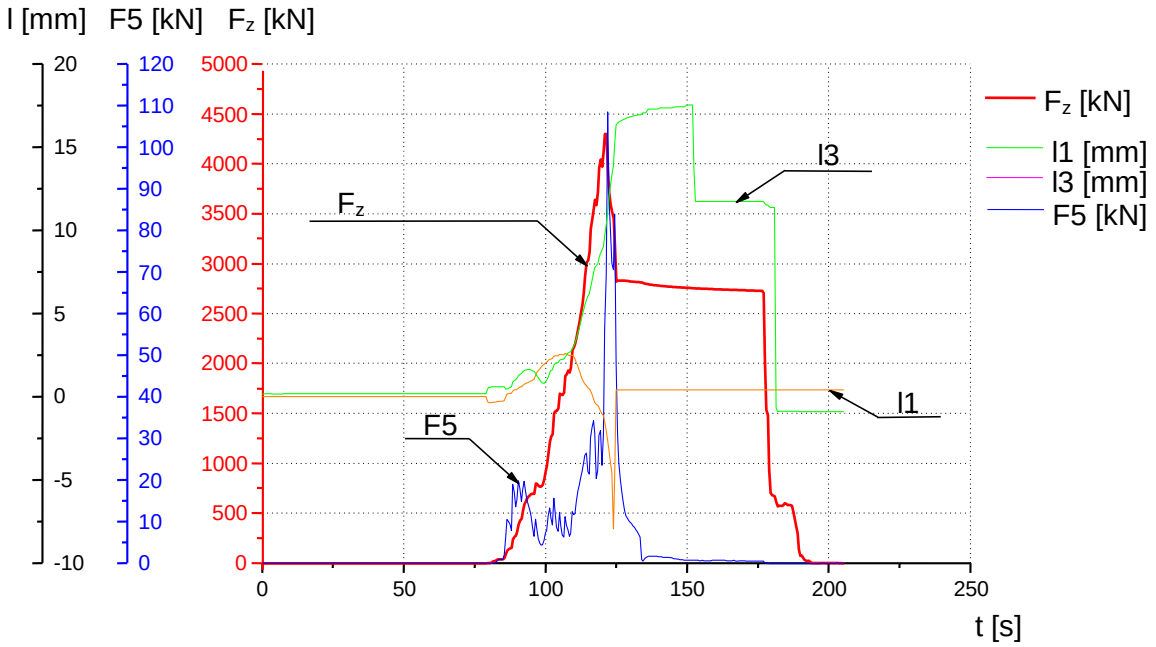

Figure 10. Time process of the measured parameters during the friction coefficient tests on a flat surface.

3. Rail testing

Bend cycles of rail sections of until they brake were the test objective. The tests procedure and their results are presented on the example of 5 samples of welded rails [8] of length 1150 mm. The test, required preparation of a special equipment shown in figure 11. Tested rail sample was placed in the equipment on a steel plate resting on four HMB, C6 strain gauge transducers with a measuring range up to 2000 kN and class 0.5.

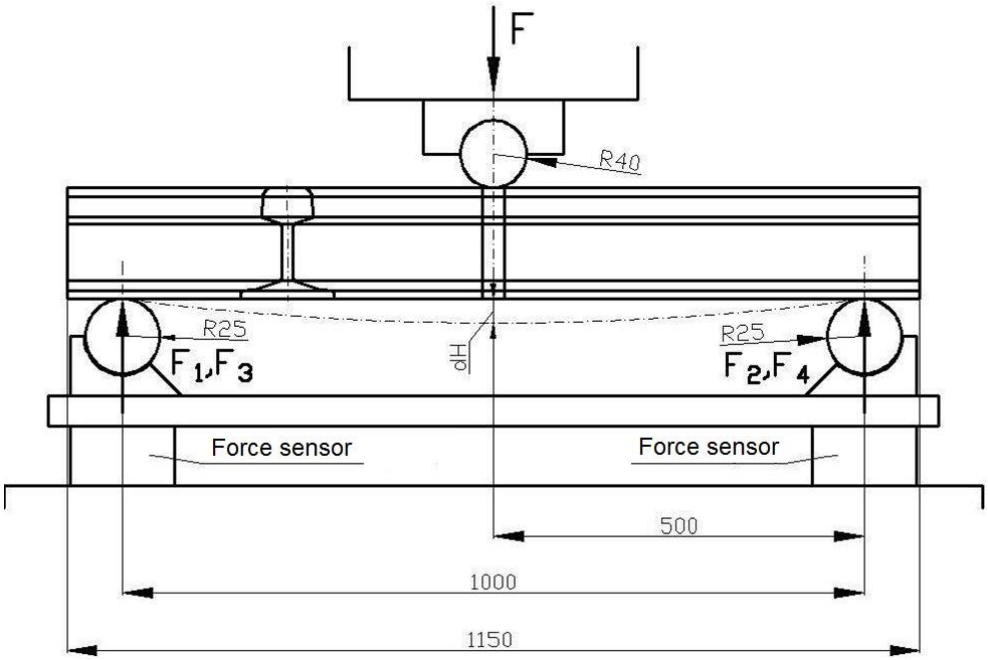

Figure 11. Equipment for bend testing of rails [9].

Transducers, together with the steel plate, the equipment and tested rails, were centrally positioned in the test stand for testing the powered roof support. By moving the roof of the stand, a vertical force bending the rail was generated. During the test, pressure force - F and deflection - dH were recorded in the middle of the sample of tested rail. The deflection was measured using the HBM type W50 displacement transducer with a measuring range of ± 50 mm and a class of 0.4.

According to the guidelines for evaluation of test results formulated by the Orderer, the tested sample meets the requirements if the value of vertical force F breaking the rail is greater than 1330 kN and the deflection inside the rail caused by destructive force is greater than 20 mm.

A sample graph of the load of tested rail sample as a function of its deflection is shown in figure 12, while the specification of maximum values of rail bending force and maximum rail deflection is presented in table 2.

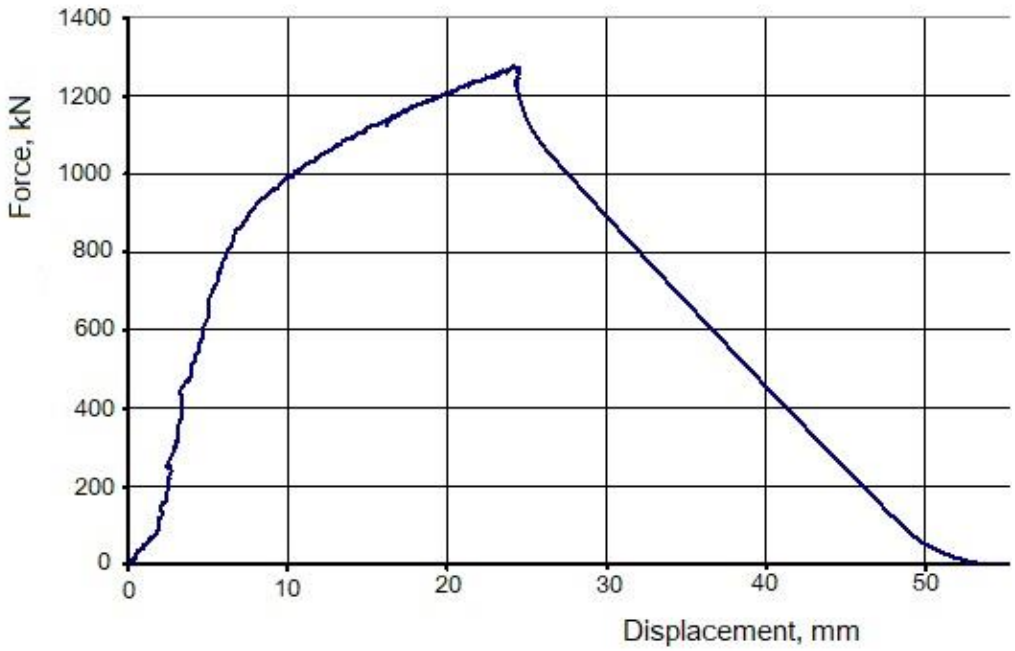

Figure 12. Changes of rail pressure force in a function of its deflection.

Table 2. List of values: maximum deflection - dH_{max} and maximum force - F_{max} obtained in the bending test of welded rails.

Sample No.	F_{max}, kN	dH_{max}, mm
1	1277,5	24,2
2	1530,4	44,0
3	1534,5	45,7
4	1226,4	21,5
5	1557,4	35,4

Table 2. shows that two of the tested rail samples do not meet the requirements formulated by the company ordering the tests. Although the maximum deflections of all tested rail samples are greater than the required value - 20 mm, in two cases the maximum force causing the rail braking is less than the required value of 1200 kN.

4. Rigidity tests of metal scaffoldings

Determination of the external scaffold load in terms of losing its rigidity was the stand tests objective. Tests procedure is presented on the example of a metal scaffolding consisting of frames and landings connected with each other by appropriate longitudinal and transversal bracing [10]. The scaffolding was installed on the fixed support or on a movable support (wheels) depending on the loading method. The total length of the tested scaffolding ranged from 5.0 to 6.0 m, depending on the length of the platforms used.

Scaffolding rigidity tests included tests of its load: by a parallel force to the platform and by a force perpendicular to the platform (figure 13 and 14). The scaffold load arrangement was in accordance with the requirements of the draft EN 12810-2: 1997-06 standard [11].

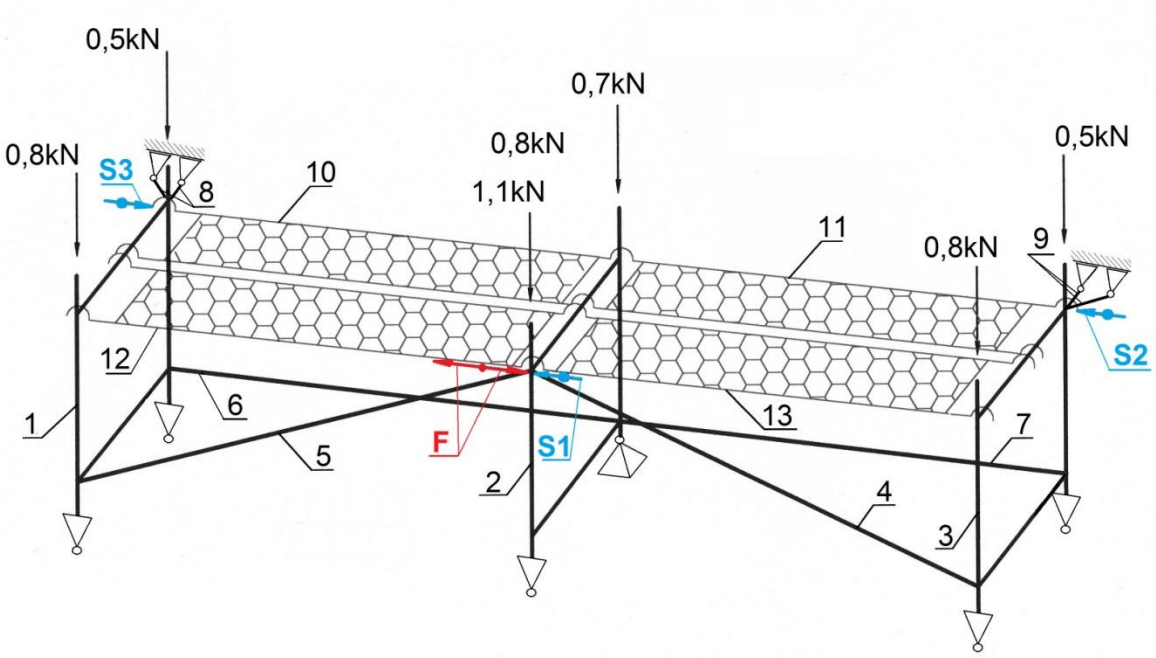

Figure 13. Scaffolding rigidity test with the force parallel to the platform – load arrangement 1, 2, 3 – scaffolding frame; 4, 5 – lateral concentration; 8, 9 - fasteners anchoring the scaffolding to the stand; 10÷13 – platform; S1, S2, S3 - directions of displacement measurement.

During the tests, the time curves of scaffolding loading force F and displacements S1, S2 and S3 of the scaffolding at three specific points were recorded. The external scaffolding load force F program included the following, sequentially implemented steps:

- load the scaffolding three times with the pushing force (under-piston area of the cylinders is supplied) and pulling force (over-piston area of the cylinders is supplied),
- three times the load of a pushing force of a specified value, and then a rapid relieving of the scaffolding,
- load of pushing force with increasing value until the first signs of the scaffolding parts destruction

Changes in the force F were realized by supplying the over-piston and under-piston area of the cylinder by a special hydraulic system. The force F was determined by means of a strain gauge force transducer, while displacement measurements were made with inductive displacement sensors. UPM-60 measuring device was used to record the measuring signals.

Sample graphs of force F in the function of displacement of point S1 for scaffolding with 3m platforms loaded with force parallel to the platform are presented in figure 15.

Figure 14. Testing the rigidity of scaffolding with force perpendicular to the platform - general view of the stand.

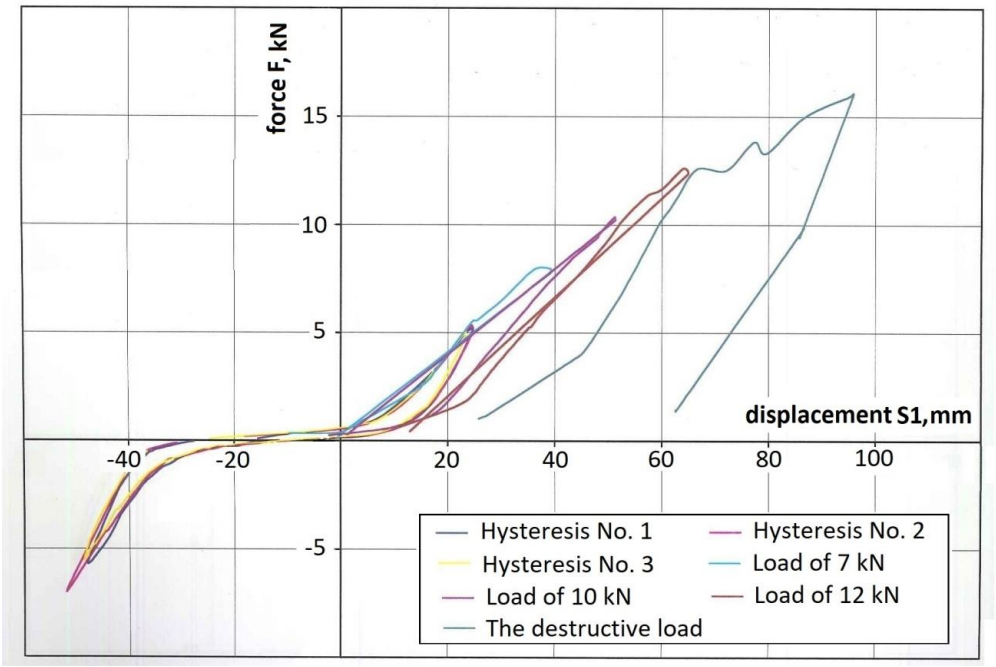

Figure 15. Graph of correlation between the force F and displacement S1 at a load parallel to the platform.

In the case of a load, the following damages caused the loss of the scaffolding rigidity:

- bending the bolting connector rod fixed at an angle of 45° to the wall of the test stand;
- deformation of the C-sections of the scaffolding frames;
- bending and deformation of the platform handles.

Initial damages resulting in the loss of rigidity of the scaffolding loaded with force perpendicular to

the platform were as follows:

- deformation of the C-sections of the scaffolding frames,
- bending and deformation of the platform handles.

The place and method of bolting the links to the walls of the stand was also found to have a significant impact on conducting the scaffolding rigidity tests. The spatial structure of the scaffolding means that the change in the method of bolting the connectors results in a significant reduction of the scaffolding's load capacity. Therefore, following the requirements of the standard [11], it is necessary to adopt the bolting connectors arrangement as close as possible to the real scaffolding work conditions, or in a result of further tests to determine the most advantageous way of bolting the scaffold in terms of its rigidity.

5. Conclusions

The necessity of experimental verification of normative requirements with regard to the functionality and strength of the powered roof support forced a development of special test stands. The overall dimensions of the powered roof support and the amount of external load carried out during the tests make very broad possibility of using these test stands.

This paper discusses the examples of using the abovementioned test stands and test equipment available in the KOMAG Institute of Mining Technology to tests other devices. The presented measurement results were used, among others, in the certification process of the tested bridge bearings. In turn, the results of rigidity tests of metal scaffoldings, in addition to verification of normative requirements, can also be used to continue cognitive research work.

The given examples of non-standard tests indicate for the possibility of a significant extension of the scope of work performed at test stands of the powered roof support.

6. References

[1] Madejczyk W 2011 *Zmechanizowane obudowy ścianowe dla warunków zagrożenia wstrząsami górotworu* ed K Stoiński (Katowice: Central Mining Institute) chapter 3 pp 39–71
[2] Zakres Akredytacji Laboratorium Badawczego Nr AB 039 wydany przez Polskie Centrum Akredytacji 01-382 Warszawa, ul. Szczotkarska 42 Wydanie nr 16. Data wydania: 13 lipca 2018 r.
[3] Madejczyk W 2011 *Maszyny Górnicze* **3** 11
[4] Niemierko A 2015 Łożyska mostowe - kontrola podczas eksploatacji *Vademecum Inżyniera. Budownictwo Mostowe* (Warszawa: WPIIB Sp. z o.o.) pp 7-10
[5] PN-EN 1337-7:2003 Łożyska konstrukcyjne Część 7: Łożyska sferyczne i cylindryczne z PTFE;
[6] PN-EN 1337-2:2005 Łożyska konstrukcyjne Część 2: Elementy ślizgowe
[7] PN-EN 1337-1:2003 Łożyska konstrukcyjne Część 1: Postanowienia ogólne
[8] Miklaszewicz I 2013 *Problemy kolejnictwa* **158** 35
[9] Warunki techniczne wykonania i odbioru zgrzein w szynach kolejowych nowych łączonych zgrzewarkami stacjonarnymi. Wymagania i badania. 2013 Załącznik do zarządzenia Nr 26/2013 Zarządu PKP z dnia 12 listopada Polskie Linie Kolejowe S.A
[10] Błazik-Borowa E 2017 *Builder* **21** (12) 48
[11] Pr EN 12810-2:1997-06 Facade scaffolds made of prefabricated elements – Part 2: Methods of particular design and assessment